Nicotiana attenuata SIPK, WIPK, NPR1, and Fatty Acid-Amino Acid Conjugates Participate in the Induction of Jasmonic Acid Biosynthesis by Affecting Early Enzymatic Steps in the Pathway[1][W][OA]

Mario Kallenbach[2], Fiammetta Alagna[2], Ian Thomas Baldwin, and Gustavo Bonaventure*

Max Planck Institute for Chemical Ecology, Department of Molecular Ecology, Jena 07745, Germany

Wounding and herbivore attack elicit the rapid (within minutes) accumulation of jasmonic acid (JA) that results from the activation of previously synthesized biosynthetic enzymes. Recently, several regulatory factors that affect JA production have been identified; however, how these regulators affect JA biosynthesis remains at present unknown. Here we demonstrate that *Nicotiana attenuata* salicylate-induced protein kinase (SIPK), wound-induced protein kinase (WIPK), nonexpressor of PR-1 (NPR1), and the insect elicitor *N*-linolenoyl-glucose (18:3-Glu) participate in mechanisms affecting early enzymatic steps of the JA biosynthesis pathway. Plants silenced in the expression of SIPK and NPR1 were affected in the initial accumulation of 13-hydroperoxy-linolenic acid (13-OOH-18:3) after wounding and 18:3-Glu elicitation by mechanisms independent of changes in 13-lipoxygenase activity. Moreover, 18:3-Glu elicited an enhanced and rapid accumulation of 13-OOH-18:3 that depended partially on SIPK and NPR1 but was independent of increased 13-lipoxygenase activity. Together, the results suggested that substrate supply for JA production was altered by 18:3-Glu elicitation and SIPK- and NPR1-mediated mechanisms. Consistent with a regulation at the level of substrate supply, we demonstrated by virus-induced gene silencing that a wound-repressed plastidial glycerolipase (NaGLA1) plays an essential role in the induction of de novo JA biosynthesis. In contrast to SIPK and NPR1, mechanisms mediated by WIPK did not affect the production of 13-OOH-18:3 but were critical to control the conversion of this precursor into 12-oxo-phytodienoic acid. These differences could be partially accounted for by reduced allene oxide synthase activity in WIPK-silenced plants.

Jasmonic acid (JA) and some of its precursors and derivatives are signal molecules that function as essential mediators of the plant's wound, antiherbivore, and antipathogen responses, as well as in growth and development (Farmer, 1994; Creelman and Mullet, 1997; Turner et al., 2002). In unelicited mature leaves, JA is maintained at very low levels, however, upon specific stimulations, its biosynthesis is induced within a few minutes (Glauser et al., 2008). This rapid biosynthetic response must result from the activation of constitutively expressed JA biosynthesis enzymes in unelicited tissue by substrate availability and/or post-translational modifications. At present, little is known about the molecular mechanisms that activate JA biosynthetic enzymes.

According to the canonical mechanism for JA biosynthesis (Vick and Zimmerman, 1983), free α-linolenic acid ($18{:}3^{\Delta 9,12,15}$, 18:3) forms 13(*S*)-hydroperoxyoctadecatrienoic acid [13S-(OOH)-18:3] by the action of 13-lipoxygenase (13-LOX) in plastids. 13S-(OOH)-18:3 is converted by allene oxide synthase (AOS) into a highly unstable allene oxide intermediate that is processed by allene oxide cyclase (AOC) to yield (9*S*,13*S*)-12-oxo-phytodienoic acid (OPDA). OPDA is transported from the plastid into the peroxisome where it is reduced by the action of OPDA reductase 3 (OPR3) and after three cycles of β-oxidation, (3*R*,7*S*)-JA is formed. Due to the large number of enzymes and different cellular compartments involved in JA biosynthesis, it is expected that the pathway is regulated at multiple steps. Resolution of the structures of the tomato (*Solanum lycopersicum*) OPR3 and Arabidopsis (*Arabidopsis thaliana*) AOC2 and ACX1 has provided insights into potential regulatory mechanisms for these enzymes (e.g. oligomerization and phosphorylation; Pedersen and Henriksen, 2005; Breithaupt et al., 2006; Hofmann et al., 2006).

The identification of two Arabidopsis plastidial glycerolipases, DAD1 and DGL (Ishiguro et al., 2001; Hyun et al., 2008), has provided genetic evidence for the importance of the release of trienoic fatty acids (FAs) from plastidial lipids in the activation of JA biosynthesis. Recently, some oxylipins have been

[1] This work was supported by the Max Planck Society.

[2] These authors contributed equally to the article.

* Corresponding author; e-mail gbonaventure@ice.mpg.de.

The author responsible for distribution of materials integral to the findings presented in this article in accordance with the policy described in the Instructions for Authors (www.plantphysiol.org) is: Gustavo Bonaventure (gbonaventure@ice.mpg.de).

[W] The online version of this article contains Web-only data.

[OA] Open Access articles can be viewed online without a subscription.

www.plantphysiol.org/cgi/doi/10.1104/pp.109.149013

found esterified to galactolipids in Arabidopsis leaves and hence it is possible that in this species preformed precursors could also supply the JA biosynthesis pathway after their release from lipids (Stelmach et al., 2001; Hisamatsu et al., 2003; Buseman et al., 2006). However, lipid-bound oxylipins are not formed in the leaves of all plant families (Böttcher and Weiler, 2007).

In *Nicotiana attenuata*, wound-induced JA production is amplified by the application of lepidopteran larvae (e.g. *Manduca sexta*) oral secretions (OS) to mechanical wounds. Major elicitors of the OS-mediated response are FA-amino acid conjugates (FACs) that are sufficient to enhance JA production in leaves of this plant species (Halitschke et al., 2001). Recently, several regulatory factors with a potential function upstream of JA biosynthesis have been identified (Ludwig et al., 2005; Takabatake et al., 2006; Schweighofer et al., 2007; Takahashi et al., 2007); however, how these regulators affect JA biosynthesis is at present unknown. For example, wounding and herbivory in *Nicotina* spp. and tomato activate the mitogen-activated protein kinases salicylate-induced protein kinase (SIPK) and wound-induced protein kinase (WIPK; Seo et al., 1999; Kandoth et al., 2007; Wu et al., 2007). When SIPK and WIPK expression is silenced in tobacco (*Nicotiana tabacum*), the plants accumulate 60% to 70% less JA than wild type after wounding or OS elicitation (Seo et al., 2007; Wu et al., 2007). Another regulatory component that affects JA production in *N. attenuata* is Nonexpressor of PR-1 (NPR1), an essential component of the salicylic acid (SA) signal transduction pathway first identified in Arabidopsis (Cao et al., 1994). *N. attenuata* NPR1-silenced plants accumulate 60% to 70% lower JA levels after elicitation than wild type (Rayapuram and Baldwin, 2007). NPR1 interacts with the JA and ethylene signaling cascades, and a cytosolic role for this factor in the regulation of JA-dependent responses/biosynthesis has been proposed (Spoel et al., 2003).

In contrast to the mechanisms acting upstream of JA biosynthesis, the mechanisms mediating downstream JA responses are better characterized (Kazan and Manners, 2008; Browse, 2009). Among the best-characterized regulators of these responses is *CORONATIVE INSENSITIVE1* (*COI1*), a gene that participates in jasmonate perception (Xie et al., 1998) and regulates gene expression through its interaction with the JASMONATE ZIM-DOMAIN repressors (Chini et al., 2007; Thines et al., 2007).

To understand the early processes regulating the activation of JA biosynthesis by wounding and FAC elicitation in *N. attenuata* leaves, we quantified the initial rates of accumulation of plastid-derived JA precursors after these stimuli in wild type and four JA-deficient genotypes previously described: ir-sipk, ir-wipk, ir-npr1, and ir-coi1 (Rayapuram and Baldwin, 2007; Paschold et al., 2008; Meldau et al., 2009). We show that SIPK, WIPK, NPR1, and FACs contribute to the activation of de novo JA biosynthesis by affecting diverse early enzymatic steps in this pathway. The identification of a plastidial glycerolipase A_1 type I family protein (GLA1) essential for JA biosynthesis pointed to this enzyme as one potential target of some of these activating mechanisms.

RESULTS

Analysis of the Initial Rates of Accumulation of JA Precursors after Wounding and FAC Elicitation

Wound- and FAC-inducible precursors of the JA biosynthetic pathway generated by the initial set of reactions in the plastid were profiled within short intervals after stimulation (0–10 min). Because JA accumulation occurs by de novo synthesis in *N. attenuata*, the rates of accumulation of these precursors within a few minutes of the wound response reflect the rapid and differential activation of specific JA biosynthetic steps when plants are subjected to different treatments. This activation therefore precedes the JA-induced transcriptional activation of JA biosynthesis genes. To study the mechanisms underlying the FAC-mediated induction of JA biosynthesis, synthetic *N*-linolenoyl-Glu (18:3-Glu) was applied onto the wounds as a single elicitor.

Because the release of trienoic FAs from membranes is considered one of the earliest regulated steps in JA biosynthesis, the absolute amounts and FA composition of four major leaf membrane glycerolipids, monogalactosyldiacylglycerol (MGDG), digalactosyldiacylglycerol, phosphatidylethanolamine, and phosphatidylcholine (PC) were first quantified within 20 min after wounding and FAC elicitation in leaves of wild-type plants. Within 10 and 20 min, JA already accumulated between 6 and 20 nmol g fresh weight $(FW)^{-1}$ (see below). Within 20 min, no significant changes in the absolute amounts of glycerolipids and their FA composition were detected (Supplemental Fig. S1a; Supplemental Table S1).

Second, levels of free FAs (FFAs) were quantified within 10 min after wounding and FAC elicitation in wild-type leaves. In unelicited tissue, total FFA accumulated to 156 ± 11 nmol g FW^{-1}, with approximately 90% of this value corresponding to saturated FFA (16:0 and 18:0) and 10% to unsaturated FFA. Saturated FFA are common constituents of epicuticular waxes and analysis of *N. attenuata* leaf waxes showed that at least 80% of total free 16:0 and 18:0 originated from the cuticle (50 ± 0.9 and 58 ± 1.3 nmol g FW^{-1}, respectively). Thus, further analysis was focused on detectable free unsaturated FA ($16{:}3^{\Delta 7,10,13}$, $18{:}1^{\Delta 9}$, $18{:}2^{\Delta 9,12}$, and $18{:}3^{\Delta 9,12,15}$). Within 10 min after the treatments, no significant changes in the levels of unsaturated FFAs were observed (Supplemental Fig. S1b), in particular of 18:3 (the major JA precursor; Fig. 1). Thus, similar to glycerolipid levels, levels of unsaturated FFA did not change significantly after wounding and FAC elicitation.

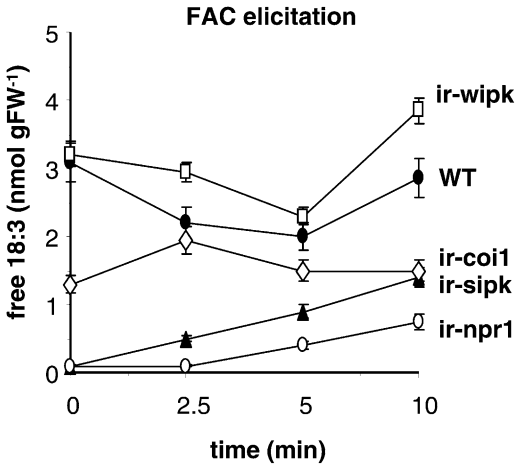

Figure 1. Levels of free 18:3 in FAC-elicited wild-type (WT) and RNAi-silenced leaves. Leaves of rosette stage wild-type, ir-sipk, ir-wipk, ir-npr1, and ir-coi1 plants were FAC elicited for different times, FFA isolated, and free 18:3 quantified. Bars = ±SE, $n = 4$. For statistical analysis, see text.

Levels of Unsaturated FFA Are Reduced in ir-sipk, ir-npr1, and ir-coi1 Plants

Total levels of unsaturated FFA were analyzed in leaves of ir-sipk, ir-wipk, ir-npr1, and ir-coi1 within 10 min after wounding and FAC elicitation. Changes in the levels of these molecules were similar between the two treatments and therefore data for FAC elicitation is only presented (Supplemental Fig. S2), and for clarity, the results corresponding to free 18:3 are presented in Figure 1. Basal levels of free 18:3 were similar to wild type in ir-wipk plants, however, reduced by approximately 10-fold in ir-sipk and ir-npr1 and by approximately 2-fold in ir-coi1 leaves (Fig. 1; $P < 0.05$, t test, wild type versus genotypes). Within 10 min after wounding and FAC elicitation, the levels of free 18:3 slowly increased in ir-sipk and ir-npr1 plants but remained nonetheless at approximately 50% and approximately 30% of wild-type levels, respectively (Fig. 1). In contrast, they remained approximately constant in ir-coi1 plants (Fig. 1). Importantly, the levels of all unsaturated FFAs were reduced in ir-sipk, ir-npr1, and ir-coi1 plants (Supplemental Fig. S2), suggesting a general alteration in FFA homeostasis in these genotypes. Quantification of MGDG, digalactosyldiacylglycerol, PC, and phosphatidylethanolamine and their FA composition in ir-sipk and ir-npr1 plants showed no significant variations compared to wild type (data not shown), suggesting that membrane glycerolipid homeostasis was not affected in these genotypes.

13-(OOH)-18:3 Production Is Differentially Induced by FAC Elicitation and Deficient in ir-sipk, ir-coi1, and ir-npr1 Plants

The levels of total free 13-(OOH)-18:3 were quantified within 10 min after wounding and FAC elicitation in wild-type and RNAi-silenced plants. In unelicited wild-type leaves, 13-(OOH)-18:3 accumulated at approximately 0.02 nmol g FW^{-1} and wounding induced a linear increase to 0.035 nmol g FW^{-1} after 5 min, the levels remaining constant for 10 min (Fig. 2A). Within 1.25 min after FAC elicitation, 13-(OOH)-18:3 levels peaked to approximately 0.07 nmol g FW^{-1} (a 2.5-fold induction compared to wounded levels at 1.25 min; $P < 0.05$, t test, wounding versus FAC elicitation) and remained at approximately 0.06 nmol g FW^{-1} within 10 min (Fig. 2A).

Similar to unsaturated FFA levels, the levels of 13-(OOH)-18:3 in ir-wipk were similar to wild type in both unelicited and elicited leaves (Fig. 2A). In contrast, basal levels of 13-(OOH)-18:3 were >2-fold lower in ir-sipk, ir-npr1, and ir-coi1 plants compared to unelicited wild-type plants (Fig. 2A; $P < 0.05$, t test, wild type versus genotypes). Moreover, after wounding, 13-(OOH)-18:3 levels were not induced in these silenced genotypes and at 10 min the levels remained >3-fold lower than in wild-type plants (Fig. 2A; $P < 0.05$, t test, wild type versus genotypes). After FAC elicitation, 13-(OOH)-18:3 levels were induced in ir-sipk, ir-npr1, and ir-coi1 plants, however, the maximum levels attained were still >2-fold lower than those in wild-type plants (Fig. 2A).

N. attenuata expresses two major 13-LOXs in leaves, LOX2 and LOX3. These two enzymes have been associated to C_6 volatile and JA biosynthesis, respectively (Halitschke et al., 2004). To quantify the fraction of total 13-(OOH)-18:3 (S + R enantiomers) originating from 13-LOX activity (S enantiomers), plants silenced in the expression of LOX3 (ir-lox3) and both LOX2 and LOX3 (ir-lox2/ir-lox3) were analyzed. ir-lox3 plants showed a significant approximately 50% reduction in basal levels of 13-(OOH)-18:3 compared to unelicited wild-type leaves (Fig. 2B; $P < 0.05$, t test, wild type versus ir-lox3) and within 10 min after wounding, the levels increased to wild-type levels (approximately 0.035 nmol g FW^{-1}), however, they were not enhanced by FAC elicitation (Fig. 2B). ir-lox2/ir-lox3 plants showed 3-fold-lower basal levels of 13-(OOH)-18:3 (approximately 0.007 nmol g FW^{-1}; $P < 0.01$, t test, wild type versus ir-lox2/ir-lox3) compared to wild type and the levels were not induced after wounding or FAC elicitation (Fig. 2B). The results indicated that LOX3 was responsible for most of the FAC-induced accumulation of 13-(OOH)-18:3 and that at least 60% to 70% of basal and almost all wound- and FAC-induced 13-(OOH)-18:3 derived from LOX2 and LOX3 activities.

OPDA Accumulation Is Compromised in ir-sipk, ir-wipk, ir-npr1, and ir-coi1 Plants

Initial changes in OPDA and dinorOPDA (dnOPDA) levels were quantified after wounding and FAC elicitation in wild-type plants and the four RNAi-silenced genotypes. In unelicited wild-type leaves, OPDA accumulated to levels <0.2 nmol g FW^{-1} and increased after 5 min of both stimuli to approximately

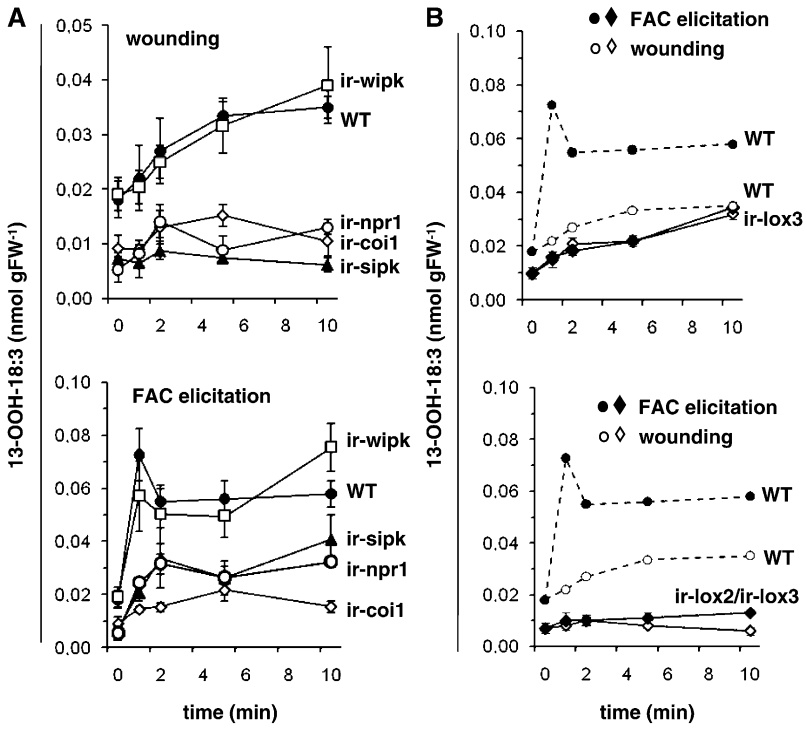

Figure 2. 13-(OOH)-18:3 levels in wild-type (WT) and RNAi-silenced plants. A, Leaves of rosette stage wild-type, ir-sipk, ir-wipk, ir-npr1, and ir-coi1 plants were wounded or FAC elicited, hydroperoxy-FA isolated, and free 13-(OOH)-18:3 quantified at different times. B, Leaves of rosette stage ir-lox3 and ir-lox2/ir-lox3 plants were treated and analyzed as above. Wild-type levels of 13-(OOH)-18:3 from A were also included (without SE) to ease the comparability. Bars = ±SE, $n = 5$. For statistical analysis, see text.

2 nmol g FW^{-1}. After wounding, the levels remained approximately constant for 10 min, however, FAC elicitation induced the accumulation of OPDA to 6 nmol g FW^{-1} at 10 min (Fig. 3A). dnOPDA could not be detected. Within 5 min after wounding or FAC elicitation, the rates of OPDA accumulation were >90% lower in ir-sipk, ir-wipk, ir-npr1, and ir-coi1 compared to wild type, and at 10 min its levels were on average 2- to 4-fold lower than in wild type (Fig. 3A; $P < 0.05$, t test, wild type versus genotypes).

We also determined whether OPDA accumulated as glycerolipid-esterified forms in *N. attenuata* leaves before and 15, 30, and 60 min after wounding and FAC elicitation. Neither OPDA nor dnOPDA could be detected in the glycolipid or polar lipid fractions whereas their levels in the neutral lipid fraction were similar to free levels in nonhydrolyzed samples (data not shown).

Quantification of JA levels within 10 min in wild-type plants showed that wounding and FAC elicitation stimulated an increase in its levels from approximately 0.25 nmol g FW^{-1} to approximately 6 nmol g FW^{-1} (Fig. 3B). Differential accumulation of JA upon FAC elicitation was detected only after 10 min (Supplemental Fig. S3) and was consistent with the sequential and differential accumulation of 13-(OOH)-18:3 and OPDA (Fig. 2A; Supplemental Fig. S3). Basal levels of JA in unelicited tissue were several-fold lower in the four silenced genotypes compared to wild type (Supplemental Fig. S4a) and within 10 min after wounding and FAC elicitation, JA accumulated at <3-fold-lower levels in the silenced genotypes (Fig. 3B; $P < 0.05$, t test, wild type versus genotypes). Basal and induced levels of SA were also quantified in unelicited and stimulated tissue of ir-sipk, ir-wipk, ir-npr1, and ir-coi1. Basal SA levels were only significantly higher in ir-sipk and ir-coi1 plants (4.5- and 3-fold, respectively, $P < 0.05$, t test, wild type versus genotypes) compared to wild type (Supplemental Fig. S4b). Within 10 min after wounding and FAC elicitation, the SA levels in the different genotypes did not change significantly compared to its basal levels (Supplemental Fig. S4b).

ir-sipk, ir-wipk, and ir-npr1 Contain Similar Levels of LOX3 Protein and 13-LOX Activity But Have Reduced AOS Activity

To determine at which level of gene expression JA biosynthesis was affected in ir-sipk, ir-wipk, ir-npr1, and ir-coi1 plants, we first determined the transcript abundance of *LOX2*, *LOX3*, *AOS*, and *AOC* by real-time quantitative PCR (RT-qPCR) in unelicited leaves of wild type and the four silenced genotypes. The results showed no significant variations in the basal levels of these transcripts between all the genotypes, suggesting that basal transcription rates (or mRNA stability) of these genes were not affected (Supplemental Fig. S5a). Second, the levels of LOX3 protein were determined by immunoblotting using an anti-NaLOX3 antibody before and after FAC elicitation. LOX3 protein amounts were similar between all the genotypes before and after the treatment (Supplemental Fig. S5b). Finally, 13-LOX and AOS activities were quantified. Basal 13-LOX activity in ir-wipk, ir-sipk, and ir-npr1 was similar to wild type, however, reduced by approximately 40% in ir-coi1 plants (Fig. 4;

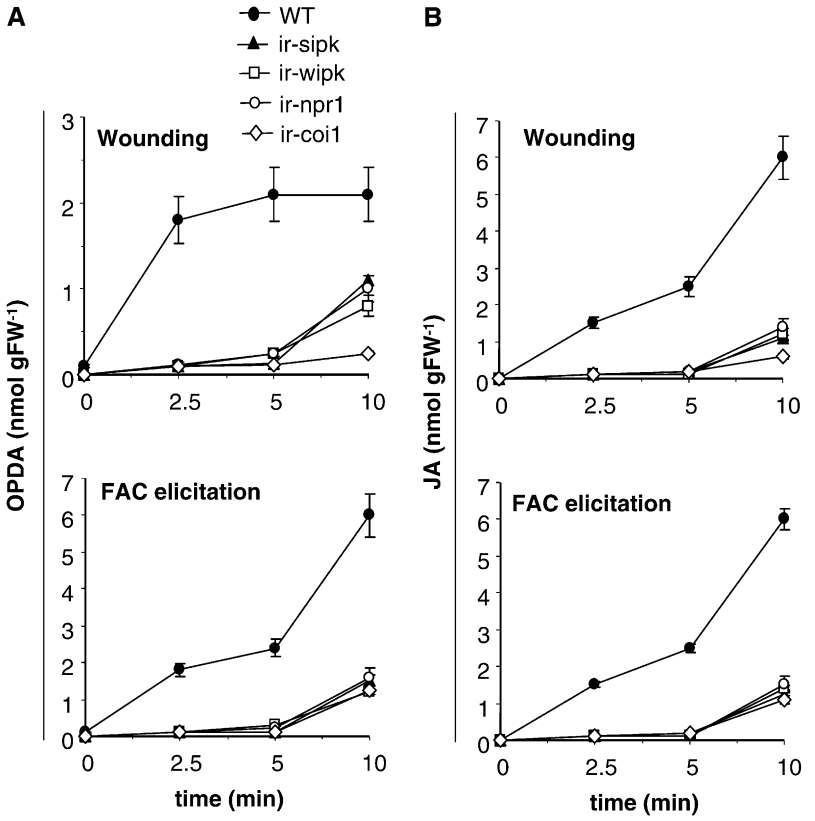

Figure 3. OPDA and JA levels in wild-type (WT) and RNAi-silenced plants. Leaves of rosette stage wild-type, ir-sipk, ir-wipk, ir-npr1, and ir-coi1 plants were wounded or FAC elicited for different times and OPDA (A) and JA (B) quantified. Bars = ±SE, $n = 5$. For statistical analysis, see text.

$P < 0.05$, t test, wild type versus genotype). AOS activity was, in contrast, significantly reduced in all silenced genotypes (by approximately 30% in ir-sipk, ir-wipk, and ir-npr1 and by 70% in ir-coi1 compared to wild type; Fig. 4; $P < 0.05$, t test, wild type versus genotype). After FAC elicitation, LOX and AOS activities remained similar to resting levels in the corresponding genotypes (Supplemental Fig. S5c).

Identification of a GLA_1-I Lipase Involved in JA Biosynthesis in *N. attenuata*

Based on the results presented above, one plausible scenario is that SIPK-, NPR1-, COI1-, and FAC-mediated mechanisms contribute to the release of 18:3 from membrane lipids and that free 18:3 is rapidly metabolized by the JA biosynthetic pathway. Thus far, only the Arabidopsis DGL and DAD1 lipases involved in wound-induced JA biosynthesis have been genetically characterized. To identify their functional homologs in *N. attenuata*, DAD1 and DGL amino acid sequences were used to search *Nicotiana* EST and UniGene databases in GenBank by basic local alignment (tblastn). Three *Nicotiana* spp. clones (DW004396, DV161431, and CK290998) gave hits with e values lower than $7e^{-22}$ when either DAD1 or DGL were used as the protein query. Based on these sequences, their respective homologs were identified in *N. attenuata*. DAD1 and DGL belong to the phospholipase-A_1 (PLA_1-I) family of phospholipases that is characterized by the presence of an N-terminal chloroplast transit peptide and a conserved lipase-3 domain with a catalytic triad consisting of Glu-His-Ser (Ryu, 2004). The three *N. attenuata* homologs presented these domains together with additional conserved structures and were tentatively named glycerolipiase A1 (GLA1; homolog to DW004396), GLA2 (homolog to DV161431), and GLA3 (homolog to CK290998).

The transcript levels of *GLA1*, *GLA2*, and *GLA3* were quantified at 0, 30, 60, and 90 min after wounding in wild type, ir-sipk, ir-npr1, and ir-coi1. ir-wipk was excluded from this analysis because it contained wild-type levels of unsaturated FFAs and 13-(OOH)-18:3. Thirty minutes after wounding, *GLA1* mRNA levels were reduced by 3- to 4-fold in wild type and the four silenced genotypes and remained at lower levels for up to 90 min (Fig. 5A). In contrast, *GLA2* transcript levels were transiently induced by 2- to 3-fold in wild type and ir-npr1 after wounding (albeit with a different kinetic) whereas not induced in ir-coi1 and ir-sipk (Fig. 5B). *GLA3* mRNA levels did not change significantly upon wounding (Fig. 5C). The kinetic of induction for these three transcripts was also quantified after FAC elicitation in wild-type plants. *GLA2* transcript levels were induced by 10-fold at 60 min whereas *GLA1* and *GLA3* transcript levels were unaffected compared to wounding (Fig. 5D).

GLA1 Is Essential for JA Biosynthesis

Virus-induced gene silencing (VIGS) was used to investigate the involvement of the three putative

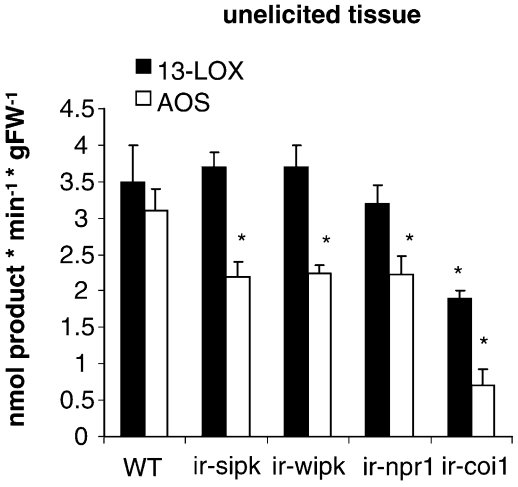

Figure 4. Analysis of 13-LOX and AOS activities. 13-LOX and AOS activities were quantified in unelicited leaves of wild-type (WT), ir-sipk, ir-wipk, ir-npr1, and ir-coi1 plants using [1-^{14}C]-18:3 or [1-^{14}C]-13-OOH-18:3 as substrates, respectively. Assays were performed in the linear phase of the reactions and ^{14}C products were extracted, separated by thin-layer chromatography, and quantified by densitometric scanning. Bars = ±SD, $n = 3$. *, See text.

GLAs in JA biosynthesis. Approximately 300 bp of their corresponding cDNAs were amplified and used for gene silencing. To ensure specific silencing, cDNA segments with low similarity between the three NaGLA cDNAs were selected (Supplemental Figure S6). Plants transformed with the empty vector (EV) were used as controls. Gene-silencing efficiency was analyzed by qRT-PCR in unwounded leaves and 60 min after FAC elicitation. In GLA1 and GLA3 VIGS-silenced plants, the corresponding mRNA levels were reduced by more than 95% and in GLA2 VIGS-silenced plants by 85% compared to EV (Supplemental Fig. S7).

First, the levels of JA and JA-Ile were quantified in EV and GLA1-, GLA2-, and GLA3-silenced plants. Leaves of EV, GLA2-, and GLA3-silenced plants accumulated similar amounts of JA and JA-Ile after FAC elicitation (Supplemental Fig. S8). In contrast, GLA1-silenced plants showed reductions of >80% in JA and JA-Ile levels at 20 min and of 75% at 1 h after FAC elicitation (Fig. 6A; $P < 0.01$, t test, EV versus GLA1). Similar results were observed after wounding alone (Supplemental Fig. S9a). Consistent with the reductions in JA and JA-Ile levels, accumulation of 13-hydroperoxy-linolenic acid (13-OOH-18:3) and OPDA was also reduced in GLA1-silenced plants compared to EV (Supplemental Fig. S9b). In contrast, the levels of unsaturated FFA (and in particular 18:3) remained similar between GLA1-silenced and EV plants after the treatments and similar to the levels in wild-type plants (data not shown).

GLA1 Is a Plastidial Glycerolipid Acyl Hydrolase with sn1 Specificity

The full-length *GLA1* cDNA was obtained by 3′ and 5′ RACE (Supplemental Fig. S10). Alignment of the full predicted amino acid sequence of GLA1 with

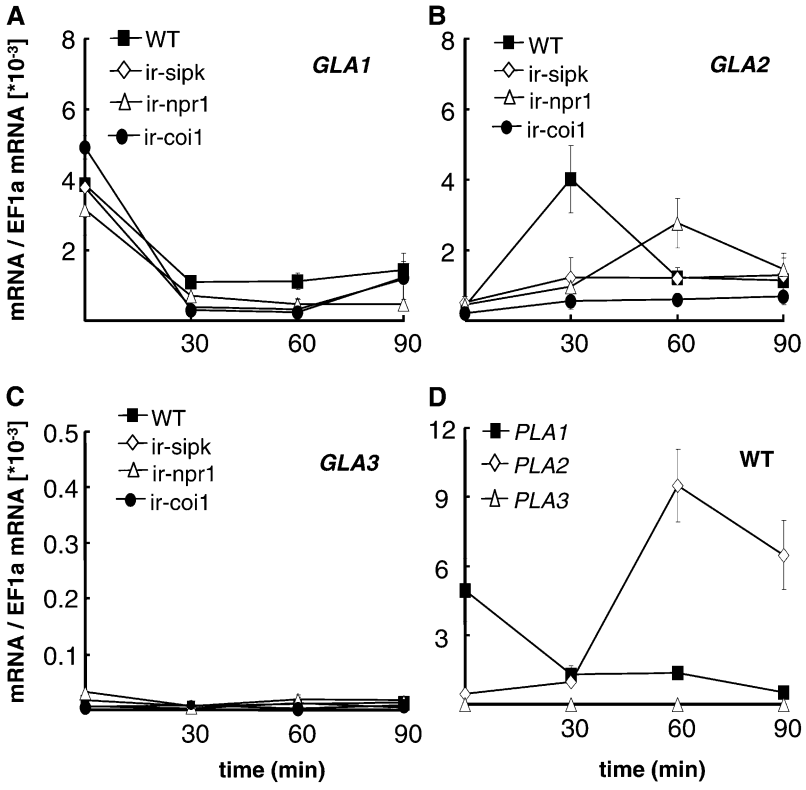

Figure 5. Analysis of GLA mRNA expression. GLA1 (A), GLA2 (B), and GLA3 (C) transcript levels were quantified by RT-qPCR in unelicited leaves of wild-type (WT), ir-sipk, ir-npr1, and ir-coi1 plants and at different times after wounding. Relative mRNA levels are expressed as the ratio of abundance of the queried mRNA over the standard (EF1a). D, Levels of all *GLA* mRNAs were quantified for different times after FAC elicitation in wild-type plants. Bars = ±SD, $n = 3$.

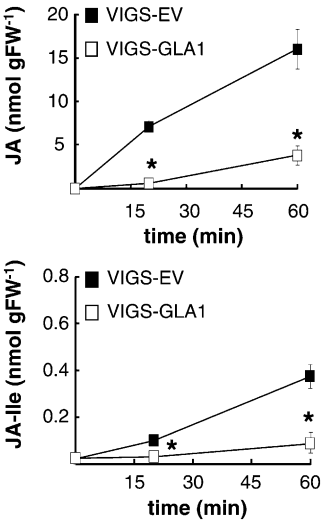

Figure 6. Quantification of JA and JA-Ile levels in plants silenced in GLA1 expression by VIGS. Control plants (VIGS-EV) and plants silenced in GLA1 expression by VIGS (VIGS-GLA1) were FAC elicited and JA and JA-Ile levels quantified in leaves after 20 and 60 min of the treatments. Bars = ±SE, $n = 8$. *, See text.

those from Arabidopsis DAD1 and DGL showed that GLA1 shared 46% identity/62% similarity and 37% identity/53% similarity with these proteins, respectively. Prediction of subcellular localization gave GLA1 a high score for plastid targeting with a predicted signal peptide of 53 residues (Supplemental Fig. S10).

To assess whether GLA1 encodes an active glycerolipid acyl hydrolase, we expressed GLA1 as a recombinant protein in bacteria and analyzed its activity toward different glycerolipid substrates. For the expression of recombinant GLA1, the predicted transit peptide was excluded to avoid the potential inhibition of lipase activity and the enzyme was fused by its N terminus to the maltose-binding protein (MBP) to promote stability (Ishiguro et al., 2001). To first evaluate if GLA1 encodes a glycerolipase type A_1, the specificity of purified MBP-GLA1 toward 1-palmitoyl-2-oleoyl-glycero-3-phosphorylcholine (POPC) was assayed. MBP-GLA1 released preferentially 16:0 from POPC whereas purified MBP showed no activity toward this substrate (Fig. 7A). MBP-GLA1 activity was also evaluated toward different glycerolipid classes, namely a phospholipid (PC), galactolipid (MGDG), and triacylglycerol (triolein). The purified enzyme hydrolyzed acyl groups at rates of approximately 2 μg h^{-1} μg $protein^{-1}$ with MGDG and PC as substrates and at approximately 1.5 μg h^{-1} μg $protein^{-1}$ with triolein as a substrate. Purified MBP did not present acyl-hydrolase activity (Fig. 7B).

To determine the subcellular localization of GLA1, the enzyme was fused to enhanced green fluorescent protein (EGFP) by its C terminus and cloned under regulation of the cauliflower mosaic virus 35S promoter (P35S:GLA1-EGFP). As controls, P35S:EGFP and a fusion EGFP protein carrying the first 273 amino acids containing the predicted plastid transit peptide of LOX3 (P35S:pLOX3-EGFP) were used. *N. attenuata* leaves were infiltrated with *Agrobacteria* carrying the corresponding constructs and EGFP expression in mesophyll cells was analyzed by laser confocal microscopy (Fig. 7C). Prior to analysis, mesophyll protoplasts were released from leaves by cell wall digestion. Protoplast transformed with EGFP showed a diffused green fluorescence characteristic of cytosolic localization that did not overlap with chlorophyll red autofluorescence. In contrast, protoplasts expressing pLOX3-EGFP and GLA1-EGFP showed colocalization

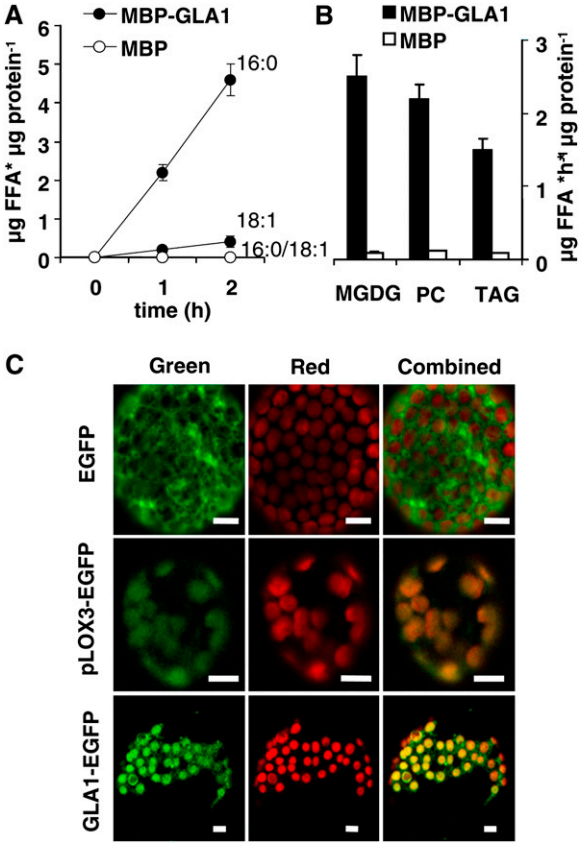

Figure 7. Characterization of GLA1 activity and subcellular localization. A, Recombinant MBP-GLA1 protein was expressed *Escherichia coli* cells and after induction and purification, enzyme activity toward POPC was assayed. Purified MBP was used as control. The assay was conducted at the optimal pH for this recombinant enzyme (pH: 6.5). Bars = ± SD, $n = 3$. B, MBP-GLA1 activity toward PC, MGDG, and triolein as substrates. Bars = ± SD, $n = 3$. C, Mesophyll protoplasts expressing P35S:EGFP, P35S:GLA1-EGFP, and P35S:pLOX3-EGFP were analyzed by laser confocal-scanning microscopy. Leaves of *N. attenuata* plants were *Agrobacteria* infiltrated and after protoplast release by cell wall digestion, mesophyll protoplasts were exited at 488 nm and emissions collected at 505 to 530 nm for EGFP and at 585 nm for chlorophyll red autofluorescence. Combined, Merged EGFP and chlorophyll autofluorescence. White scale bar: 10 μm.

of green and red fluorescences, consistent with their predicted plastidial localization.

DISCUSSION

GLA1 Participates in the Activation of JA Biosynthesis in *N. attenuata* Leaves

The absence of massive glycerolipid degradation and release of FFA after mechanical damage contrasted with some previous studies performed in other plant species where substantial breakdown of glycerolipids and release of FFA was detected after wounding (Conconi et al., 1996; Ryu and Wang, 1998). These differences are most likely a result of the different methods used to mechanically damage the leaf (crushing leaf tissue versus punctured wounds) and therefore differences in cell disruption and uncontrolled hydrolysis of membrane lipids. The absolute amounts of 18:3 in galactolipids were on average 1.3 μmol g FW^{-1}, more than 100-fold the amount of substrate needed to supply JA biosynthesis within 10 min (6–20 nmol g FW^{-1} g FW; Fig. 3B). Therefore, specific supply of 18:3 for JA biosynthesis within this time frame was not expected to cause substantial changes in the FA composition of major plastidial lipids. In contrast, however, significant changes in the total levels of free 18:3 (which accumulated to approximately 3 nmol g FW^{-1}; Fig. 1) were expected, since OPDA and JA accumulated to comparable levels (Fig. 3B) within 10 min after wounding and FAC elicitation, respectively. Unexpectedly, the levels of this FFA did not change significantly within this period. Consistent with this observation, plants silenced in GLA1 expression showed no significant changes in the levels of free 18:3 and other unsaturated FFAs compared to control EV plants after wounding and FAC elicitation, however, 13-OOH, OPDA, JA, and JA-Ile production was strongly reduced in these silenced plants (Fig. 6; Supplemental Fig. S9). These results, together with the localization of GLA1 in the chloroplasts, provided strong evidence for a rapid and specific supply of 18:3 for JA biosynthesis via GLA1. We cannot completely rule out, however, the possibility that the effect of GLA1 on JA biosynthesis is indirect.

Similar to Arabidopsis DGL and DAD1, GLA1 is a member of the lipase A_1-I family and is expressed in vegetative tissues in the absence of wounding (Ishiguro et al., 2001; Hyun et al., 2008). Also, similar to DAD1 and DGL, GLA1 hydrolyzed both PC and MGDG, however in contrast to DAD1 (which hydrolyzes PC more efficiently; Ishiguro et al., 2001) and DGL (which hydrolyzes galactolipids more efficiently; Hyun et al., 2008) the activity of GLA1 toward these substrates was similar. Because GLA1 localizes to the plastids, it is likely that galactolipids are the major in vivo substrates for this lipase. Whereas *DAD1* and *DGL* transcripts are induced by wounding (Ishiguro et al., 2001; Hyun et al., 2008), *GLA1* mRNA levels were repressed by this stimulus. This repression may reflect variations in the regulation of some JA biosynthetic genes in different plant species and underscore the fact that changes in transcript accumulation did not correlate with GLA1 function.

FAC Elicitation, SIPK, NPR1, and COI1 Regulate Early Enzymatic Steps in the JA Biosynthetic Pathway

Free 13-(OOH)-18:3 levels increased after wounding and more rapidly after FAC elicitation in wild-type plants (Fig. 2). The absolute amounts remained, however, low (0.01–0.08 nmol g FW^{-1}) in agreement with previous studies, suggesting a rapid utilization of this precursor (Weichert et al., 1999). After FAC elicitation, 13-LOX activity and LOX3 protein levels were not increased compared to unelicited tissue in wild-type plants (Fig. 4; Supplemental Fig. S5b), suggesting that the enhanced accumulation of 13-(OOH)-18:3 after this stimulus was the result of an increase in 18:3 supply rather than the differential activation of LOX3. One possible scenario is the differential activation of GLA1 via FAC-mediated mechanisms, however, this hypothesis requires further experimentation and is the focus of future studies.

Basal levels of FFA (including 18:3) were reduced >10-fold in ir-sipk and ir-npr1 plants compared to wild type (Fig. 1) and increased after wounding and FAC elicitation, remaining nonetheless lower than in wild type after the same treatments. These results suggested that homeostatic mechanisms that maintain wild-type levels of unsaturated FFA were affected in these silenced plants. Whether this global reduction in FFA levels was directly connected to a reduced supply of 18:3 for JA production in these genotypes is at present unknown. However, as the initial accumulation of 13-OOH-18:3 was strongly reduced after wounding and FAC elicitation in ir-sipk and ir-npr1 plants (Fig. 2A) independently of reductions in 13-LOX activity and LOX3 protein levels (Fig. 4; Supplemental Fig. S5b), we concluded that in ir-sipk and ir-npr1 plants, the supply of 18:3 for JA biosynthesis was affected. Thus, at present there are two potential explanations: (1) that a global suppression of FFA levels affects (by still unknown mechanisms) the supply of 18:3 for JA production in ir-sipk and ir-npr1 plants, or (2) that SIPK and NPR1 influences by independent mechanisms both, the regulation of homeostatic levels of FFA and the specific supply of 18:3 for JA production. Thus, although speculative at this point, we propose that the supply of 18:3 via NaGLA1 may be one regulatory step by which SIPK- and NPR1-mediated mechanisms contribute to the activation of JA biosynthesis.

ir-coi1 plants had approximately 50% reduced basal levels of FFAs compared to wild type (Supplemental Figs. S1b and S2) and in contrast to ir-sipk and ir-npr1 plants, FFA levels did not increase after wounding and FAC elicitation. ir-coi1 plants also accumulated lower levels of 13-OOH-18:3 after these treatments, however,

in contrast to ir-sipk and ir-npr1 plants, in ir-coi1 plants had 40% reduced levels of 13-LOX activity (Fig. 4). Thus, the results suggested that in the latter genotype, the initial 13-(OOH)-18:3 accumulation was primarily limited by reduced 13-LOX activity.

SIPK, WIPK, NPR1, and COI1-Mediated Mechanisms Participate in the Regulation of OPDA Synthesis

The mRNA levels of AOS and AOC in unelicited tissue of ir-sipk, ir-wipk, ir-npr1, and ir-coi1 were similar to those of wild-type plants, indicating that their rates of transcription/turnover were not affected (Supplemental Fig. S5a). However, AOS activity was reduced by 30% in ir-sipk, ir-npr1, and ir-wipk and by 70% in ir-coi1 plants, suggesting that these differences were the result of posttranscriptional processes.

Although ir-wipk plants contained wild-type levels of free 18:3 and accumulated wild-type levels of 13-(OOH)-18:3 after elicitation, the rate of OPDA synthesis was reduced by more than 90% within 5 min of the response (Fig. 3A). Thus, the reduced AOS activity in ir-wipk plants indicated that WIPK-mediated mechanisms are important to maintain basal AOS activity and suggested that this enzyme's activity limited OPDA accumulation after elicitation. However, since the reduction in the initial rates of OPDA accumulation were bigger than the expected by the 30% reduction in AOS activity, additional enzymatic steps may also be affected in ir-wipk plants. For example, evidence from the crystal structure of Arabidopsis AOC2 suggests that this enzyme is regulated posttranslationally by oligomerization (Hofmann et al., 2006). Thus, although speculative at this point, we do not rule out the possibility that AOC may also be a target of WIPK-mediated mechanisms.

CONCLUSION

Upon wounding and herbivory, cellular mechanisms quickly convey the signal to the plastid to activate constitutively expressed enzymes and to start the immediate production of JA. How plants convey the primary stress signal to activate these enzymes remain at present largely unknown. Due to the large number of enzymes and different cellular compartments involved in JA biosynthesis, it is expected that the pathway is regulated at multiple steps. Consistent with this hypothesis, recent evidence indicates that OPR3, AOC2, and ACX1 are subjected to regulation (Pedersen and Henriksen, 2005; Breithaupt et al., 2006; Hofmann et al., 2006). The recent identification of different regulatory factors that affect JA accumulation (Ludwig et al., 2005; Takabatake et al., 2006; Schweighofer et al., 2007; Takahashi et al., 2007) is also consistent with a complex network of signals inducing JA biosynthesis (Browse, 2009). In this study we demonstrated that signal transduction mechanisms involving SIPK, WIPK, NPR1, and the insect elicitor 18:3-Glu affect different early JA biosynthetic steps. We propose that after wounding, FAC perception differentially stimulate the supply of 18:3 for JA biosynthesis and that SIPK- and NPR1-mediated mechanisms also stimulate this biochemical step. The identification of GLA1 as a lipase essential for JA biosynthesis suggested that the above-mentioned factors may exert their effects via the regulation of this enzyme's activity. In contrast, WIPK-mediated mechanisms operate in the control of the biosynthetic steps that convert 13-(OOH)-18:3 into OPDA. This control is at least partially executed by the regulation of AOS activity. Further elucidation of the mechanisms affecting enzyme activity would provide critical information on the understanding of how primary stress signals are translated into the activation of JA biosynthetic enzymes.

MATERIALS AND METHODS

Please refer to online Supplemental Experimental Procedures S1 for further details.

Plant Growth and Treatments

Seeds of the 22nd generation of an inbred line of *Nicotiana attenuata* plants were used as the wild-type genotype in all experiments. Plants were grown at 26°C to 28°C under 16 h of light. For all experiments, leaves at nodes +1, +2, and +3 of rosette stage (40-d-old) plants were used. Wounding was performed by rolling a fabric pattern wheel three times on each side of the midvein. The wounds were immediately supplied with either 10 μL of 0.02% (v/v) Tween 20/water (solvent control) or 10 μL of synthetic 18:3-Glu (0.03 nmol/μL in 0.02% [v/v] Tween 20/water). Tissue was collected and immediately frozen in liquid nitrogen for subsequent analysis.

Oxylipin Analysis

Hydroperoxy FAs were extracted with the chloroform-methanol method. Briefly, approximately 1 g of frozen leaf material was homogenized in 10 mL glass tubes containing 3.75 mL of ice-cold 2/1 (v/v) chloroform/methanol spiked with 5 ng of 15-hydroperoxy-eicosadienoic acid (Cayman Chemicals). After addition of 1.25 mL chloroform and 1 mL water, samples were vortexed and phases separated. The organic phase was collected and the water phase reextracted with 3 mL hexane. Hexane and chloroform fractions were combined, the solvent evaporated under a stream of nitrogen, and samples reconstituted in 70% (v/v) methanol/water and analyzed by liquid chromatography-(ESI)-tandem mass spectrometry (see online Supplemental Experimental Procedures S1). Commercial 13S-(OOH)-18:3 and 9(R/S)-OOH-18:3 were used as standards (Cayman Chemicals). For analysis of JA, JA-Ile, OPDA, and SA, approximately 0.1 g of frozen leaf material was homogenized in FastPrep tubes containing 1 g of FastPrep matrix (Bio 101) and 1 mL ethyl acetate spiked with 100 ng of [9,10-^{2}H]-dihydro-JA, [$^{13}C_4$]-SA, and [$^{13}C_6$]-JA-Ile. Homogenates were centrifuged for 10 min at 4°C, the organic phase collected, and plant material reextracted with 0.5 mL ethyl acetate. Organic phases were combined and the samples evaporated to dryness. The dry residue was reconstituted in 0.2 mL of 70% (v/v) methanol/water and analyzed by liquid chromatography-(ESI)-tandem mass spectrometry (see online Supplemental Experimental Procedures S1).

Identification of Homologs of DAD1 and DGL

The amino acid sequences from Arabidopsis (*Arabidopsis thaliana*) DAD1 (AtPLA$_1$-Iβ1) and DGL (AtPLA$_1$-Iα1) were used to search *Nicotiana* EST and RefSeq databases by basic local alignment (BLAST) in GenBank. Specific primers (Supplemental Table S2) were designed based on *Nicotiana* CK290998, DV161431, and DW004396 sequences to PCR amplify their respective homo-

logs in *N. attenuata*. PCR products were obtained using *N. attenuata* leaf cDNA as template and cloned into pGEM-T easy vector (Promega) and sequenced. The corresponding *N. attenuata* sequences were named GLA1 (homolog to DW004396), GLA2 (homolog to DV161431), and GLA3 (homolog to CK290998; see accession numbers listed below).

VIGS

A VIGS system based on *Tobacco rattle virus* was used (Ratcliff et al., 2001) adapted for *N. attenuata* according to Saedler and Baldwin (2004). cDNA fragments of GLA1, GLA2, and GLA3 (Supplemental Fig. S6) were amplified by PCR using plasmids carrying their respective cDNA sequences (see section above) as templates and specific primers (Supplemental Table S2). After digestion with *Bam*HI and *Sal*I and gel purification, the PCR products were subcloned into pTV100 to form pTV-LIP1, 2, and 3. *Agrobacterium tumefaciens* strain GV3101 carrying these gene-specific constructs were coinoculated with *Agrobacteria* carrying pBINTRA6 into *N. attenuata* leaves according to Saedler and Baldwin (2004). Plants were analyzed 15 d after inoculation.

In Vitro Quantification of GLA1 Activity

Soybean (*Glycine max*) PC, wheat (*Triticum aestivum*) MGDG, and triolein (Sigma) and POPC (Matreya) were used as substrates. Lipids were emulsified by sonication in 0.2% (v/v) Triton X-100 at 1 μg/μL. Reaction buffer (50 mM K-phosphate [pH 6.5], 0.2% [v/v] Triton X-100), 40 μg of substrate, and 16 μg of purified protein (either MBP or MBP-GLA1) in a final volume of 100 μL were used for the assays. The reaction was carried out at 30°C for 1 and 2 h and stopped by the addition of 2 mL of chloroform. Lipids were extracted twice with chloroform and FFA purification and analysis was performed by thin-layer chromatography and gas chromatography-mass spectrometry as described for plant material.

Subcellular Localization GLA1

N. attenuata leaves were infiltrated with *A. tumefaciens* GV3101 carrying pCAMBIA-1201 vectors expressing P35S:GLA1-EGFP, P35S:pLOX3-EGFP, and P35S:EGFP (see online Supplemental Experimental Procedures). Infiltration was performed as indicated in the VIGS section above. Four days after infiltration, leaves were collected and protoplast isolated by floating leaf strips on 0.2% (w/v) bovine serum albumin, 2% (w/v) cellulase, 1% (w/v) macerozyme, 400 mM mannitol, 8 mM $CaCl_2$, and 5 mM MES (pH 5.6) for 3 h at 25°C with gentle shaking. Protoplasts were collected by centrifugation (100*g*) for 5 min and immediately used for microscopy. Confocal laser-scanning microscopy was performed using a LSM 510 Meta microscope (Carl Zeiss) equipped with an argon laser. Samples were excited at 488 nm and emissions collected with 505 to 530 nm and 585 nm filters for EGFP and chlorophyll red autofluorescence, respectively. Images were processed using the image software supplied by the microscope manufacturer (Carl Zeiss).

Sequence data from this article can be found in the GenBank/EMBL data libraries under accession numbers: GLA1 (FJ821553), GLA2 (FJ821554), GLA3 (FJ821555), LOX3 (AY254349), LOX2 (AY254348), AOS (AJ295274), AOC (EF467332), DAD1 (Atg244810), and DGL (At1g05800).

Supplemental Data

The following materials are available in the online version of this article.

Supplemental Figure S1. Membrane glycerolipid and unsaturated FFA levels in wild-type leaves.

Supplemental Figure S2. Unsaturated FFA levels in RNAi-silenced plants.

Supplemental Figure S3. OPDA and JA levels in wild-type plants within 20 min of induction.

Supplemental Figure S4. Basal levels of JA and basal and induced levels of SA.

Supplemental Figure S5. RT-qPCR and LOX3 protein levels.

Supplemental Figure S6. Alignment of GLA sequences used for VIGS.

Supplemental Figure S7. Quantification of GLA mRNA levels in VIGS-silenced plants.

Supplemental Figure S8. Quantification of JA and JA-Ile levels in GLA2- and GLA3-silenced plants.

Supplemental Figure S9. Quantification of 13-OOH-18:3, OPDA, JA, and JA-Ile levels in GLA1-silenced plants.

Supplemental Figure S10. Full-length mRNA and amino acid sequences of GLA1.

Supplemental Table S1. FA composition of membrane glycerolipids in wild-type leaves.

Supplemental Table S2. Primer sequences.

Supplemental Experimental Procedures S1. Additional methods.

ACKNOWLEDGMENTS

We thank Ewald Grosse-Wilde for his assistance with the laser-confocal microscope and Silke Allmann for providing ir-lox2/ir-lox3 seeds.

Received October 8, 2009; accepted November 3, 2009; published November 6, 2009.

LITERATURE CITED

Böttcher C, Weiler E (2007) Cyclo-oxylipin-galactolipids in plants: occurrence and dynamics. Planta **226:** 629–637

Breithaupt C, Kurzbauer R, Lilie H, Schaller A, Strassner J, Huber R, MacHeroux P, Clausen T (2006) Crystal structure of 12-oxophytodienoate reductase 3 from tomato: self-inhibition by dimerization. Proc Natl Acad Sci USA **103:** 14337–14342

Browse J (2009) Jasmonate passes muster: a receptor and targets for the defense hormone. Annu Rev Plant Biol **60:** 183–205

Buseman CM, Tamura P, Sparks AA, Baughman EJ, Maatta S, Zhao J, Roth MR, Esch SW, Shah J, Williams TD (2006) Wounding stimulates the accumulation of glycerolipids containing oxophytodienoic acid and dinor-oxophytodienoic acid in Arabidopsis leaves. Plant Physiol **142:** 28–39

Cao H, Bowling SA, Gordon AS, Dong X (1994) Characterization of an *Arabidopsis* mutant that is nonresponsive to inducers of systemic acquired resistance. Plant Cell **6:** 1583–1592

Chini A, Fonseca S, Fernández G, Adie B, Chico J, Lorenzo O, García-Casado G, López-Vidriero I, Lozano F, Ponce M, et al (2007) The JAZ family of repressors is the missing link in jasmonate signalling. Nature **448:** 666–671

Conconi A, Miquel M, Browse JA, Ryan CA (1996) Intracellular levels of free linolenic and linoleic acids increase in tomato leaves in response to wounding. Plant Physiol **111:** 797–803

Creelman RA, Mullet JE (1997) Biosynthesis and action of jasmonates in plants. Annu Rev Plant Physiol Plant Mol Biol **48:** 355–381

Farmer EE (1994) Fatty-acid signaling in plants and their associated microorganisms. Plant Mol Biol **26:** 1423–1437

Glauser G, Grata E, Dubugnon L, Rudaz S, Farmer EE, Wolfender JL (2008) Spatial and temporal dynamics of jasmonate synthesis and accumulation in Arabidopsis in response to wounding. J Biol Chem **283:** 16400–16407

Halitschke R, Schittko U, Pohnert G, Boland W, Baldwin IT (2001) Molecular interactions between the specialist herbivore *Manduca sexta* (Lepidoptera, Sphingidae) and its natural host *Nicotiana attenuata*. III. Fatty acid-amino acid conjugates in herbivore oral secretions are necessary and sufficient for herbivore-specific plant responses. Plant Physiol **125:** 711–717

Halitschke R, Ziegler J, Keinanen M, Baldwin IT (2004) Silencing of hydroperoxide lyase and allene oxide synthase reveals substrate and defense signaling crosstalk in Nicotiana attenuata. Plant J **40:** 35–46

Hisamatsu Y, Goto N, Hasegawa K, Shigemori H (2003) Arabidopsides A and B, two new oxylipins from Arabidopsis thaliana. Tetrahedron Lett **44:** 5553–5556

Hofmann E, Zerbe P, Schaller F (2006) The crystal structure of *Arabidopsis thaliana* allene oxide cyclase: insights into the oxylipin cyclization reaction. Plant Cell **18:** 3201–3217

Hyun Y, Choi S, Hwang HJ, Yu J, Nam SJ, Ko J, Park JY, Seo YS, Kim EY, Ryu SB, et al (2008) Cooperation and functional diversification of two closely related galactolipase genes for jasmonate biosynthesis. Dev Cell **14:** 183–192

Ishiguro S, Kawai-Oda A, Ueda J, Nishida I, Okada K (2001) The DEFECTIVE IN ANTHER DEHISCIENCE gene encodes a novel phospholipase A1 catalyzing the initial step of jasmonic acid biosynthesis, which synchronizes pollen maturation, anther dehiscence, and flower opening in *Arabidopsis*. Plant Cell **13:** 2191–2209

Kandoth PK, Ranf S, Pancholi SS, Jayanty S, Walla MD, Miller W, Howe GA, Lincoln DE, Stratmann JW (2007) Tomato MAPKs LeMPK1, LeMPK2, and LeMPK3 function in the systemin-mediated defense response against herbivorous insects. Proc Natl Acad Sci USA **104:** 12205–12210

Kazan K, Manners J (2008) Jasmonate signaling: toward an integrated view. Plant Physiol **146:** 1459–1468

Ludwig AA, Saitoh H, Felix G, Freymark G, Miersch O, Wasternack C, Boller T, Jones JDG, Romeis T (2005) Ethylene-mediated cross-talk between calcium-dependent protein kinase and MAPK signaling controls stress responses in plants. Proc Natl Acad Sci USA **102:** 10736–10741

Meldau S, Wu JQ, Baldwin IT (2009) Silencing two herbivory-activated MAP kinases, SIPK and WIPK, does not increase Nicotiana attenuata's susceptibility to herbivores in the glasshouse and in nature. New Phytol **181:** 161–173

Paschold A, Bonaventure G, Kant MR, Baldwin IT (2008) Jasmonate perception regulates jasmonate biosynthesis and JA-Ile metabolism: the case of COI1 in Nicotiana attenuata. Plant Cell Physiol **49:** 1165–1175

Pedersen L, Henriksen A (2005) Acyl-CoA oxidase 1 from Arabidopsis thaliana: structure of a key enzyme in plant lipid metabolism. J Mol Biol **345:** 487–500

Ratcliff F, Martin-Hernandez AM, Baulcombe DC (2001) Technical advance: tobacco rattle virus as a vector for analysis of gene function by silencing. Plant J **25:** 237–245

Rayapuram C, Baldwin IT (2007) Increased SA in NPR1-silenced plants antagonizes JA and JA-dependent direct and indirect defenses in herbivore-attacked Nicotiana attenuata in nature. Plant J **52:** 700–715

Ryu SB (2004) Phospholipid-derived signaling mediated by phospholipase A in plants. Trends Plant Sci **9:** 229–235

Ryu SB, Wang X (1998) Increase in free linolenic and linoleic acids associated with phospholipase D-mediated hydrolysis of phospholipids in wounded castor bean leaves. Biochim Biophys Acta **1393:** 193–202

Saedler R, Baldwin IT (2004) Virus-induced gene silencing of jasmonate-induced direct defences, nicotine and trypsin proteinase-inhibitors in Nicotiana attenuata. J Exp Bot **55:** 151–157

Schweighofer A, Kazanaviciute V, Scheikl E, Teige M, Doczi R, Hirt H, Schwanninger M, Kant M, Schuurink R, Mauch F, et al (2007) The PP2C-type phosphatase AP2C1, which negatively regulates MPK4 and MPK6, modulates innate immunity, jasmonic acid, and ethylene levels in *Arabidopsis*. Plant Cell **19:** 2213–2224

Seo S, Katou S, Seto H, Gomi K, Ohashi Y (2007) The mitogen-activated protein kinases WIPK and SIPK regulate the levels of jasmonic and salicylic acids in wounded tobacco plants. Plant J **49:** 899–909

Seo S, Sano H, Ohashi Y (1999) Jasmonate-based wound signal transduction requires activation of WIPK, a tobacco mitogen-activated protein kinase. Plant Cell **11:** 289–298

Spoel SH, Koornneef A, Claessens S, Korzelius JP, Van Pelt JA, Mueller MJ, Buchala AJ, Metraux JP, Brown R, Kazan K, et al (2003) NPR1 modulates cross-talk between salicylate-and jasmonate-dependent defense pathways through a novel function in the cytosol. Plant Cell **15:** 760–770

Stelmach B, Müller A, Hennig P, Gebhardt S, Schubert-Zsilavecz M, Weiler E (2001) A novel class of oxylipins, sn1-O-(12-oxophytodienoyl)-sn2-O-(hexadecatrienoyl)-monogalactosyl diglyceride, from Arabidopsis thaliana. J Biol Chem **276:** 12832–12838

Takabatake R, Seo S, Ito N, Gotoh Y, Mitsuhara I, Ohashi Y (2006) Involvement of wound-induced receptor-like protein kinase in wound signal transduction in tobacco plants. Plant J **47:** 249–257

Takahashi F, Yoshida R, Ichimura K, Mizoguchi T, Seo S, Yonezawa M, Maruyama K, Yamaguchi-Shinozaki K, Shinozaki K (2007) The mitogen-activated protein kinase cascade MKK3-MPK6 is an important part of the jasmonate signal transduction pathway in *Arabidopsis*. Plant Cell **19:** 805–818

Thines B, Katsir L, Melotto M, Niu Y, Mandaokar A, Liu GH, Nomura K, He SY, Howe GA, Browse J (2007) JAZ repressor proteins are targets of the SCFCO11 complex during jasmonate signalling. Nature **448:** 661–665

Turner JG, Ellis C, Devoto A (2002) The jasmonate signal pathway. Plant Cell **14:** S153–S164

Vick BA, Zimmerman DC (1983) The biosynthesis of jasmonic acid: a physiological role for plant lipoxygenase. Biochem Biophys Res Commun **111:** 470–477

Weichert H, Stenzel I, Berndt E, Wasternack C, Feussner I (1999) Metabolic profiling of oxylipins upon salicylate treatment in barley leaves-preferential induction of the reductase pathway by salicylate. FEBS Lett **464:** 133–137

Wu JQ, Hettenhausen C, Meldau S, Baldwin IT (2007) Herbivory rapidly activates MAPK signaling in attacked and unattacked leaf regions but not between leaves of *Nicotiana attenuata*. Plant Cell **19:** 1096–1122

Xie DX, Feys BF, James S, Nieto-Rostro M, Turner JG (1998) COI1: an Arabidopsis gene required for jasmonate-regulated defense and fertility. Science **280:** 1091–1094